

Identification in source apportionment using geometry

Bora Jin, Abhirup Datta

Department of Biostatistics, Johns Hopkins University

Abstract

Source apportionment analysis, which aims to quantify the attribution of observed concentrations of multiple air pollutants to specific sources, can be formulated as a non-negative matrix factorization (NMF) problem. However, NMF is non-unique and typically relies on unverifiable assumptions such as sparsity and uninterpretable scalings. In this manuscript, we establish identifiability of the source attribution percentage matrix under much weaker and more realistic conditions. We introduce the population-level estimand for this matrix, and show that it is scale-invariant and identifiable even when the NMF factors are not. Viewing the data as a point cloud in a conical hull, we show that a geometric estimator of the source attribution percentage matrix is consistent without any sparsity or parametric distributional assumptions, and while accommodating spatio-temporal dependence. Numerical experiments corroborate the theory.

Keywords: Convex geometry; Non-negative matrix factorization; Source apportionment; Source attribution percentage matrix; Stationary ergodic processes; Statistical identifiability.

1 Introduction

Environmental pollutants in an area are typically produced by multiple sources, including industry, traffic, residential heating, construction, and natural events. An important scientific and policy question then arises about which sources drive each pollutant. Source apportionment answers this question by quantifying the attribution of observed pollutant concentrations to underlying sources. Let $Y \in \mathbb{R}^{n \times J}$ be the observed concentration matrix, where n is the number of samples and J is the number of pollutants. In source apportionment, with K sources, $Y \approx WH$ with $W \in \mathbb{R}^{n \times K}$ as source emissions and $H \in \mathbb{R}^{K \times J}$ as per-unit source profiles. Because Y , W , and H correspond to concentrations, they must be non-negative, reducing this to a non-negative matrix factorization (NMF) problem. In the air quality literature, related ideas often appeared as multivariate receptor models. Positive Matrix Factorization is a leading method (Paatero and Tapper, 1994). Other notable approaches include geometric ideas (Henry, 1997), Bayesian methods (Hackstadt and Peng, 2014), and models with temporal (Park et al., 2001) or spatial correlation (Jun and Park, 2013). See Krall and Chang (2019) for a review.

Geometric perspectives have also been influential in NMF, viewing the samples $\{Y_i^\top = W_i^\top H : i = 1, \dots, n\}$ as a point cloud in a simplicial cone with rows of H as corners. Under separability, where each source is represented by at least one ‘pure’ observation, N-FINDR (Winter, 1999) estimate the convex hull to recover source profiles. Vertex Component Analysis (Nascimento and Dias, 2005) and XRAY (Kumar et al., 2013) also exploit the geometry of convex cones. In source apportionment, UNMIX (Henry, 1997) estimates the edges of the multivariate data cloud and interprets them as source profiles.

NMF is generally non-identifiable and subject to the classic factor indeterminacy. For example, $Y = WH$ admits equivalent representations of the form $(WD)(D^{-1}H)$ for any positive diagonal matrix D . Thus, simple least squares based methods cannot uniquely identify the two factors. Identifiability is often enforced by additional constraints such as structured zero patterns (Fritzilas et al., 2010) or stochasticity constraints (Du et al., 2016) on rows or columns in W or H . Sug Park et al. (2002) establishes identifiability assuming both exact sparsity of W and an assumed scaling of H . Other forms of structural assumptions include exact (sparse) separability (Winter, 1999; Donoho and Stodden, 2003; Nascimento and Dias, 2005) or sufficiently scattered factors (Fu et al., 2018).

Naive application of NMF identification strategies to source apportionment is inadequate. Deterministic assumptions on the matrices are unlikely to hold exactly and lack physical justification in environmental applications. Misspecified sparsity patterns can bias results, and fitted factors are highly sensitive to such choices (Viana et al., 2008). Moreover, existing identifiability results for NMF still only ensure uniqueness up to scaling of the factor matrices, leaving ambiguity in interpretation. In source apportionment, the rows of H are commonly interpreted as source profiles (Krall and Chang, 2019). As the scaling of H is not uniquely identifiable, a common strategy is to normalize the rows of H to sum to one. Although widely adopted (Manousakas et al., 2025), such a practice yields incoherent fractions when pollutants are measured in incompatible units, assumes that the pollutant list is exhaustive, neglects the contribution magnitudes encoded in W , and cannot directly answer which sources drive each pollutant.

Most NMF identifiability studies also lack a stochastic data-generating model and therefore provide no framework for analyzing statistical properties of the resulting estimators. They also do not consider spatio-temporal dependence, which is typical of air pollution concentration data. Finally, their theory often speaks to global optima, while their algorithms may only reach local solutions (Gillis, 2017).

We address these gaps in the identifiability theory of source apportionment by introducing a stochastic data-generating framework and a population-level inferential target, the source attribution percentage matrix. This estimand directly answers the policy question of which sources are the principal contributors to each pollutant in the area. Each entry has natural physical meaning as the percentage of the expected concentration of a pollutant attributable to a source. This matrix Φ allows comparison across pollutants measured in different units, is grounded at the population level through expectations rather than individual realizations, and, crucially, is invariant to rescaling of H , overcoming the limitations of profile-based interpretations.

We then provide, to our knowledge, the most general conditions for identifiability of Φ . Using the point-cloud geometry, we give an explicit algorithm to consistently estimate Φ under a probabilistic form of separability, weaker than the deterministic conditions standard in NMF theory. No true sparsity or fixed scaling of H is assumed. We also avoid parametric distributional assumptions on source emissions; allowing them to be just stationary and ergodic processes to accommodate spatio-temporal dependence. Our results make the case for using geometric methods in source apportionment.

2 Problem formulation

2.1 Premise of source apportionment

Let Y_{ij} denote the concentration of the j th pollutant in the i th data record, where i corresponds to a time point or a space-and-time combination. With K sources, we model

$$Y_{ij} = \sum_{k=1}^K W_{ik} H_{kj} \quad (1)$$

where $H_{kj} \geq 0$ denotes the concentration of pollutant j per unit of emissions from source k , and $W_{ik} \geq 0$ denotes the emission volume from that source in record i . We leave ‘one unit’ vague as we will show that our estimand is invariant to the unit choice.

Let $Y_i = (Y_{i1}, \dots, Y_{iJ})^\top \in \mathbb{R}_+^J$, $W_i = (W_{i1}, \dots, W_{iK})^\top \in \mathbb{R}_+^K$, and $H = (H_{kj}) \in \mathbb{R}_+^{K \times J}$. Then $Y_i^\top = W_i^\top H$, and stacking the n records gives $Y = WH$. Row-normalizing H to form a profile matrix is hard to interpret when pollutants use incompatible units. For example, suppose the true profile of a source (one row of H) is $1000\mu\text{gm}^{-3}$ of PM_{2.5} (fine particulate matter) and 100 ppb of CO (carbon monoxide) per unit emission. After normalization, that row of H becomes $(\frac{10}{11}, \frac{1}{11})$. If PM_{2.5} was measured in mgm^{-3} , the same profile becomes $(\frac{1}{101}, \frac{100}{101})$. Thus a unit change can completely flip dominance of a pollutant in a source profile making normalized profiles uninterpretable.

In source apportionment, we advocate focusing on the percentages of each pollutant attributable to each source, rather than inferring on the factor matrices W and H . We now define this quantity and show subsequently that it can be consistently estimated under mild assumptions using geometric methods. Note that $\sum_{i=1}^n Y_{ij}$ denotes the total concentration of pollutant j in the data and $\sum_{i=1}^n W_{ik} H_{kj}$ is the total arising from source k . Then the fraction of total concentration of pollutant j attributable to source k is

$$\frac{\sum_{i=1}^n W_{ik} H_{kj}}{\sum_{i=1}^n Y_{ij}}, \quad (2)$$

which we believe corresponds to the ‘percent of species’ output produced by the PMF software (EPA, 2015). This quantity is also routinely reported in other studies (Hagan et al., 2019), although we have not found this exact formula explicitly documented.

We define a population-level analog of the ratio in (2). Under a stochastic framework for the emissions W and mild conditions formally defined later, $\frac{1}{n} \sum_{i=1}^n W_{ik} \rightarrow \mu_k$ where $\mu_k = \mathbb{E}(W_{ik})$ is the expected emission volume from the k th source. Then, $\frac{1}{n} \sum_{i=1}^n Y_{ij} \rightarrow \sum_{\ell=1}^K \mu_\ell H_{\ell j}$. So, the ratio in (2) is the sample version of the population-level quantity

$$\phi_{kj} = \frac{\mu_k H_{kj}}{\sum_{\ell=1}^K \mu_\ell H_{\ell j}}. \quad (3)$$

The $K \times J$ column-stochastic matrix $\Phi = (\phi_{kj})$ is our estimand, representing the fraction of the total concentration of pollutant j attributed to source k . We call Φ the source attribution percentage matrix, following the PMF terminology.

2.2 Scale invariance

Section 2.1 noted that the row-normalized version of H often used in source apportionment analysis is not invariant to column-wise scaling of H , i.e., pollutant specific unit changes. In contrast, our estimand Φ is. From equation (3), scaling column j of Y by $\sigma_j > 0$ gives $\phi_{kj}^{(\text{scaled})} =$

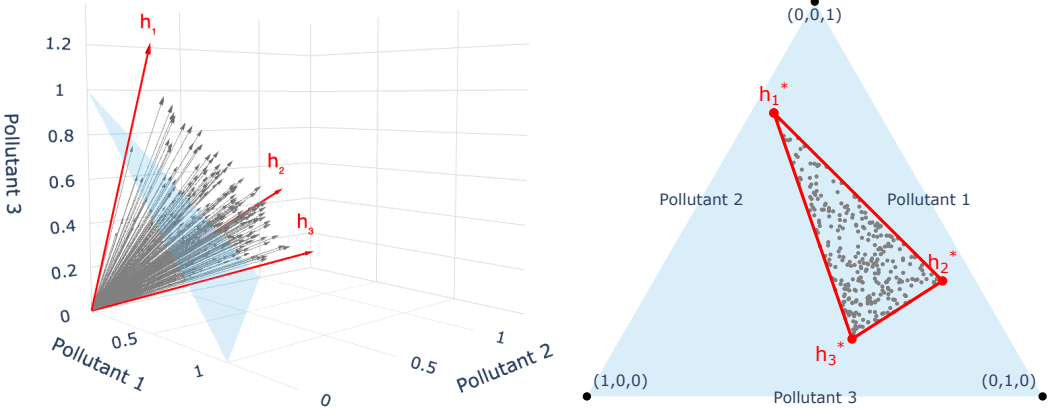


Figure 1: Geometric representation of multipollutant source apportionment

$\mu_k H_{kj} \sigma_j / (\sum_{\ell=1}^K \mu_\ell H_{\ell j} \sigma_j) = \phi_{kj}$. Equivalently, if $Y = WH$ is rewritten as $Y = \tilde{W}\tilde{H}$ where $\tilde{W} = WD$ and $\tilde{H} = D^{-1}H$ for some diagonal matrix D with positive entries, then Φ computed from (W, H) is same as that from (\tilde{W}, \tilde{H}) . This scale invariance is expected and desirable: unit changes do not affect source attributions.

2.3 Statistical identifiability

Beyond scale invariance, Φ is statistically identifiable. Our argument uses conical geometry of the data cloud. We begin by introducing the main geometric concepts.

Definition 1 (Conical hull and extremal rays). *Let $\mathcal{V} = \{v_1, \dots, v_M\} \subseteq \mathbb{R}_+^d$. Then $\text{cone}(\mathcal{V}) = \{\sum_{m=1}^M \alpha_m v_m : \alpha_m \geq 0, v_m \in \mathcal{V}\}$ is its conical hull. A set $\mathcal{U} = \{u_1, \dots, u_R\} \subseteq \text{cone}(\mathcal{V})$ is said to be a set of representatives of extremal rays of $\text{cone}(\mathcal{V})$ if (i) $\text{cone}(\mathcal{U}) = \text{cone}(\mathcal{V})$; (ii) $u_i \in \mathcal{U}$ implies that $cu_i \notin \mathcal{U}$ for any $c \neq 1$ and $c > 0$; and (iii) no u_i can be written as a non-negative linear combination of $\{u_j : j \neq i\}$.*

The extremal rays are the corner lines (the one-dimensional faces) of the polyhedral cone $\text{cone}(\mathcal{V})$. None of these rays can be expressed as a non-negative linear combination of the others, and thus they form the minimal generating set whose conical hull is $\text{cone}(\mathcal{V})$.

Set $\mathcal{H} = \{h_1, \dots, h_K\}$ where h_k^T is the k th row vector of H . Without loss of generality, we can assume that none of the h_k 's are non-negative linear combinations of the other $h_{k'}$; otherwise we can remove that source. If Y_i is generated according to (1), each vector $Y_i = \sum_{k=1}^K W_{ik} h_k$ lies within $\text{cone}(\mathcal{H})$. With sufficiently rich sampling, the cone should fill up and one should be able to identify the corner vectors h_k (up to scalar multiples) from the data. Figure 1 (left) illustrates the point cloud (grey vectors) lying in the cone of three extremal rays (red vectors). To visualize the identification of these extremal rays, we intersect the cone with the canonical simplex and show the barycentric projections in Figure 1 (right). The resulting scatter is contained within the triangle with vertices h_1^*, h_2^*, h_3^* , where each h_k^* is the normalized version of h_k . With sufficiently dense sampling inside this triangle, the vertices can be identified, allowing recovery of the scaled h_k 's.

To prove that Φ is uniquely determined across different NMF representations of Y , we specify data-generating assumptions.

Assumption 1 (Ergodicity and stationarity of source emissions). *$\{W_i\}_{i \geq 1}$ is an ergodic stationary process on \mathbb{R}_+^K with marginal distribution \mathbb{P}_W supported on a set $\mathbb{S}_W \subseteq \mathbb{R}_+^K$ and with finite mean $\mu = \mathbb{E}(W_i)$.*

This allows temporal or spatio-temporal dependence in $\{W_i\}_{i \geq 1}$ without any parametric restrictions on \mathbb{P}_W or on the dependence structure of the processes. This assumption covers many standard time-series models, including stable autoregressive (AR), moving-average (MA), and ARMA processes with a stable AR component.

We further impose the following condition on \mathbb{S}_W :

Assumption 2 (Probabilistic separability). *There exist constants $c_k > 0$ such that $c_k e_k \in \mathbb{S}_W$ for every $k = 1, \dots, K$, where e_k is the k th canonical basis vector in \mathbb{R}^K .*

This assumption ensures that, with positive probability, the process $\{W_i\}_{i \geq 1}$ produces realizations where one coordinate dominates. Unlike the deterministic separability used in NMF (e.g., Donoho and Stodden, 2003) which requires exact zeros in the W matrix, this probabilistic version only requires the support of the distribution of W to contain points arbitrarily close to $c_k e_k$. This relaxation is well suited for source apportionment, where it is plausible for one source to occasionally dominate but unrealistic for all others to be completely absent. Under these two assumptions, we state the identifiability result.

Theorem 1 (Statistical identifiability). *Suppose each data point Y_i admits two NMF representations $Y_i^\top = W_i^\top H = \widetilde{W}_i^\top \widetilde{H}$, where H and \widetilde{H} are $K \times J$ non-negative matrices, $\{W_i\}_{i \geq 1}$ and $\{\widetilde{W}_i\}_{i \geq 1}$ are K -dimensional processes satisfying Assumptions 1 – 2, and at least one of H or \widetilde{H} has full row rank. Let Φ , defined in (3), denote the percentage matrix derived from \mathbb{P}_W and H , and let $\widetilde{\Phi}$ be the analogous quantity based on $\mathbb{P}_{\widetilde{W}}$ and \widetilde{H} . Then $\widetilde{\Phi} = \Phi$ up to a permutation of rows.*

Hence Φ is well defined and statistically identifiable (up to reordering of the sources), even though the NMF representation of the data matrix Y need not be unique.

3 Consistent estimation

3.1 Convex hull and vertex estimation

We now provide an algorithm to consistently estimate Φ . Figure 1 shows how the point cloud Y increasingly resembles the cone generated by \mathcal{H} as the sample size grows, enabling identification of its extremal rays, or equivalently, the row vectors of H . Because these rays determine only directions, each row of H is identified up to a positive scalar row multipliers. However, from Theorem 2, Φ is invariant to row-scaling of H . We will thus use a row-normalized H to consistently estimate Φ .

Let $d_k > 0$ be the sum of the entries in h_k , and set $D = \text{diag}(d_1, \dots, d_K)$. Define the row-stochastic matrix $H^* = D^{-1}H$. Write $\widetilde{W} = WD$ and let $r = (r_1, \dots, r_n)^\top = \widetilde{W}1_K$ be the vector of row sums of \widetilde{W} where 1_K is the K -vector of ones. Set $W_i^* = \widetilde{W}_i/r_i$ and form W^* by stacking the row vectors $W_i^{*\top}$. Then $Y = (\text{diag}(r))W^*H^* = (\text{diag}(r))Y^*$ where $Y^* = W^*H^*$. Both W^* and H^* are row-stochastic, so Y^* is also row-stochastic. Moreover, $Y1_J = r$, so r can be computed directly from the observed data Y . We therefore estimate H^* based on the row-normalized data $Y^* = (\text{diag}(r))^{-1}Y$.

Let $\Delta^{J-1} = \{v \in \mathbb{R}^J : v_j \geq 0, \sum_{j=1}^J v_j = 1\}$ denote the canonical simplex in \mathbb{R}^J . Each Y_i^* lies in Δ^{J-1} and is a convex combination of the rows h_k^* of H^* with weights W_{ik}^* . Hence, every Y_i^* belongs to the convex hull generated by the rows of H^* , $\text{conv}(\mathcal{H}^*) = \text{conv}\{h_1^*, \dots, h_K^*\}$. Geometrically, $\text{conv}(\mathcal{H}^*)$ is a convex polytope and can be viewed as the intersection of $\text{cone}(\mathcal{H})$ with Δ^{K-1} , as illustrated in Figure 1. When W_i^* lies near a vertex of Δ^{K-1} , the corresponding Y_i^* is close to one of the vertices h_k^* . As \mathbb{P}_{W^*} has support near every corner of Δ^{K-1} , as n increases the sample

$\{Y_1^*, \dots, Y_n^*\}$ will reveal all vertices of $\text{conv}(\mathcal{H}^*)$, which are exactly the rows of H^* . Thus H^* can be estimated by identifying the extreme points of the point cloud formed by Y^* . Formally, the result below states that the sample convex hull of Y^* consistently estimates $\text{conv}(\mathcal{H}^*)$.

Theorem 2 (Hausdorff consistency of the sample convex hull). *Suppose $Y_i^\top = W_i^\top H$ where H is a $K \times J$ non-negative matrix of full row rank, and $\{W_i\}_{i \geq 1}$ is a K -dimensional process satisfying Assumptions 1 – 2. Let Y_i^* and H^* be as defined above. Then, almost surely,*

$$d_{\text{Haus}}(\text{conv}\{Y_1^*, \dots, Y_n^*\}, \text{conv}\{h_1^*, \dots, h_K^*\}) \rightarrow 0$$

where d_{Haus} is the Hausdorff distance.

Previous consistency results for sample convex hulls assume independent and identically distributed observations (Brunel, 2019). Separately, work in topological data analysis considers dependent stationary sequences, establishing Hausdorff convergence (Kallel and Louhichi, 2024) and deriving convergence rates in expectation (Louhichi, 2025). However, these results require additional regularity beyond stationarity and ergodicity such as a positive minimal index or β -mixing. Neither line of research has explored implications of their theoretical results for source apportionment. Theorem 2 fills this gap by proving convex hull consistency for dependent data only under stationarity and ergodicity, realistic assumptions in the context of source apportionment.

Theorem 2 guarantees hull consistency. Our goal is to actually recover H^* on way to estimating Φ . Note that as the true H^* has K rows, the set $\text{conv}(\mathcal{H}^*)$ is a K -vertex polytope. As the sample hull converges to this polytope, a well chosen set of K points from the sample hull should converge to the rows of H^* . We use a simple but empirically effective maximum-volume K -polytope estimator. The next result shows its consistency. Other rules of selecting K vertices from the sample hull, such as minimizing the Hausdorff distance of the resulting K -polytope to the sample hull, would also be consistent.

Corollary 1 (Consistency of the maximum-volume K -vertex estimator). *Under the conditions of Theorem 2, let $\widehat{\mathcal{H}}_n^* = \{\widehat{h}_1^*, \dots, \widehat{h}_K^*\} \subset S_n$ be the K -point subset of $S_n = \text{conv}\{Y_1^*, \dots, Y_n^*\}$ that corresponds to the K -polytope with maximum volume. Then $d_{\text{Haus}}(\{\widehat{h}_{n,1}^*, \dots, \widehat{h}_{n,K}^*\}, \{h_1^*, \dots, h_K^*\}) \rightarrow 0$ almost surely.*

Corollary 1 gives a consistent estimate of H^* , the row-normalized version of H . However, as discussed before, H^* may not be scientifically interpretable when the pollutants are measured in incompatible units. Next, we estimate Φ using this estimate of H^* .

3.2 Estimation of factor means and the percentage matrix

Since $Y = WH = \widetilde{W}H^*$ and Φ is invariant to different NMF factorizations by Theorem 1, the source attributions from equation (3) become

$$\phi_{kj} = \frac{\widetilde{\mu}_k H_{kj}^*}{\sum_{\ell=1}^K \widetilde{\mu}_\ell H_{\ell j}^*}, \quad \widetilde{\mu}_k = \mathbb{E}(\widetilde{W}_{ik}). \quad (4)$$

The following proposition presents a consistent estimator of $\widetilde{\mu}$.

Proposition 1. *Assume the setting of Theorem 2. Let \widehat{H}^* be a row-permuted estimator with $\widehat{H}^* \rightarrow_p H^*$. Write $\bar{Y}_n = \sum_{i=1}^n Y_i/n$ for the column mean of Y and $\bar{r}_n = \bar{Y}_n^\top 1_J$ for its total. Let $\widehat{H}_{\text{aug}}^* = [\widehat{H}^* \ 1_K]$. Define the affine right inverse $R(\widehat{H}^*) = \widehat{H}_{\text{aug}}^{*\top} (\widehat{H}_{\text{aug}}^* \widehat{H}_{\text{aug}}^{*\top})^+ \in \mathbb{R}^{(J+1) \times K}$, where $(\cdot)^+$ denotes the Moore-Penrose inverse. Let $\tilde{m}_n^T = [\bar{Y}_n^\top \ \bar{r}_n] R(\widehat{H}^*) \in \mathbb{R}^{1 \times K}$. Then $\tilde{m}_n \rightarrow_p \widetilde{\mu} = \mathbb{E}(\widetilde{W}_1)$. If $\widehat{H}^* \rightarrow_{a.s.} H^*$, then $\tilde{m}_n \rightarrow_{a.s.} \widetilde{\mu}$.*

Algorithm 1 SOURCE ATTRIBUTION PERCENTAGE MATRIX ESTIMATION

Input: $Y \in \mathbb{R}_+^{n \times J}$, number of sources $K < J$.

Output: $\hat{\Phi}$

- 1: **Row normalization:** set $r \leftarrow Y1_J$ and $Y^* \leftarrow (\text{diag}(r))^{-1} Y$.
- 2: **Sample hull:** compute convex hull S_n of the rows of Y^* .
- 3: **Max-volume subset:** set $\hat{\mathcal{H}}_n^* = \arg \max_{\{x_1, \dots, x_K\} \subset S_n} \text{vol}_{K-1}(\text{conv}\{x_1, \dots, x_K\})$ and let \hat{H}^* be the matrix with these vectors as rows.
- 4: **Affine right-inverse:** $R \leftarrow \hat{H}_{\text{aug}}^{*T} (\hat{H}_{\text{aug}}^* \hat{H}_{\text{aug}}^{*T})^+$.
- 5: **Sample mean:** $\tilde{m}_n^T \leftarrow [\bar{Y}_n^T \quad \bar{r}_n] R$.
- 6: **Source attributions:** $\hat{\Phi} \leftarrow \text{eq (4)} \text{ with } \tilde{m}_n \text{ and } \hat{H}^*$.
- 7: **Return** $\hat{\Phi}$.

Combining the strongly consistent estimators \hat{H}^* and \tilde{m}_n in equation (4) yields a strongly consistent estimator of Φ up to row permutations. This completes construction of a consistent estimator of the source attribution percentages. The complete procedure is summarized in Algorithm 1 while a more detailed algorithm is in Supplemental Section S2. Extensive numerical experiments in Supplementary Section S3 confirm that our estimator of Φ becomes increasingly accurate as sample size grows.

4 Discussion

We break the myth that source apportionment results can only be understood assuming sparsity or scaling assumptions. Moving away from interpreting non-unique NMF matrices, we define a population-level estimand for the matrix of the percentages of each pollutant concentration attributable to each source. We show that this quantity is scale invariant, statistically identifiable, and consistently estimable using a simple algorithm. The results make a strong case for use of geometric ideas in source apportionment.

This study focused on resolving the identifiability issues in source apportionment, several aspects of this topic merit further study. It is important extend the framework to missing data and measurement errors, develop more statistically and computationally efficient algorithms, and pursue data driven inference on the number of sources.

Supplementary materials for “Identification in source apportionment using geometry”

Bora Jin, Abhirup Datta

Department of Biostatistics, Johns Hopkins University

S1 Proofs

Before proving Theorem 1, we state a standard result for ergodic processes. The proof included here for completeness.

Lemma S1. *Let $\{X_t\}_{t \in \mathbb{N}}$ be a stationary ergodic process on a separable metric space (X, d) with support set S , i.e., for every $a \in S$ and every ball $\epsilon > 0$ one has $P(X_1 \in B_\epsilon(a)) > 0$ for a ball $B_\epsilon(a)$ around a . Then for any $a \in S$ there exists a random subsequence $\{t_k\}_{k \geq 1}$ such that $X_{t_k} \rightarrow a$ almost surely.*

Proof. Fix $a \in S$. For $n \geq 1$ set $A_n = B_{1/n}(a)$ and define $I_t^{(n)} = I\{X_t \in A_n\}$, where $I\{\cdot\}$ denotes the indicator function. By stationarity, $\mathbb{E}(I_t^{(n)}) = P(X_1 \in A_n) > 0$ for each n . By Birkhoff’s ergodic theorem,

$$\frac{1}{N} \sum_{t=1}^N I_t^{(n)} \rightarrow P(X_1 \in A_n) \quad \text{almost surely.}$$

Hence for each n the set $\{t \in \mathbb{N} : X_t \in A_n\}$ is infinite with probability one. Construct inductively $t_1 < t_2 < \dots$ by choosing t_k so that $X_{t_k} \in A_k$. Then $d(X_{t_k}, a) \leq 1/k$ for all k with probability one, which implies $X_{t_k} \rightarrow a$ almost surely. \square

Proof of Theorem 1. For notational simplicity we drop tildes and write $\widetilde{W}_i = Z_i$, $\widetilde{H} = G$, $\widetilde{\mu} = \eta$, and $\widetilde{\Phi} = \Psi$. Let g_k^\top denote the k th row of G .

Fix $k \in \{1, \dots, K\}$. Because $c_k e_k \in \mathbb{S}_Z$ and $\{Z_i\}_{i \geq 1}$ is ergodic, Lemma S1 provides a subsequence $\{Z_{i(m)}\}$ with $Z_{i(m)} \rightarrow c_k e_k$ almost surely as $m \rightarrow \infty$. Since $Y_{i(m)}^\top = Z_{i(m)}^\top G$, it follows that $Y_{i(m)}^\top \rightarrow c_k g_k^\top$ almost surely. But $Y_i^\top = W_i^\top H$ as well, so we have $W_{i(m)}^\top H \rightarrow c_k g_k^\top$, implying $c_k g_k^\top$ is the limit of a sequence of vectors in the cone generated by H . The cone being closed, implies that $c_k g_k$, and consequently g_k , lies in it. Hence, $g_k^\top = a_k^\top H$ for some $a_k \in \mathbb{R}_+^K$. Letting A be the $K \times K$ matrix with rows a_k^\top gives

$$G = AH, \quad A \geq 0 \text{ (entrywise non-negative)}.$$

By symmetry (interchanging (W, H) and (Z, G)), there exists $B \geq 0$ with

$$H = BG.$$

Without loss of generality, take H to be of full row rank. Combining the relations between H and G yields

$$H = BG = BAH.$$

As H is full row rank, $BA = I_K$, so A is invertible and $A^{-1} = B$ has non-negative entries. A non-negative matrix with a non-negative inverse must be monomial (Berman and Plemmons, 1979), i.e. $A = PD$ with a permutation matrix P and a positive diagonal matrix $D = \text{diag}(d_1, \dots, d_K)$. Therefore, $G = AH = PDH$. After reordering rows (permuting sources) we may take $P = I_K$,

giving $G = DH$ and thus $g_k = d_k h_k$. Each row of G coincides with a row of H up to a positive scalar.

Taking expectations of $Y_i^\top = W_i^\top H = Z_i^\top G = Z_i^\top DH$ gives $\mathbb{E}(W_i^\top)H = \mathbb{E}(Z_i^\top)DH$. Since H has full row rank, this implies $\mathbb{E}(W_i^\top) = \mathbb{E}(Z_i^\top)D$, so $\mu_k = d_k \eta_k$. Finally,

$$\psi_{kj} = \frac{\eta_k G_{kj}}{\sum_{\ell=1}^K \eta_\ell G_{\ell j}} = \frac{(\mu_k/d_k)(d_k H_{kj})}{\sum_{\ell=1}^K (\mu_\ell/d_\ell)(d_\ell H_{\ell j})} = \phi_{kj},$$

establishing $\Psi = \Phi$. \square

Proof of Theorem 2. Let $\mathcal{H}^* = \{h_1^*, \dots, h_K^*\}$ and let \mathcal{A} be the support of \mathbb{P}_{W^*} . Recall that every observation satisfies $Y_i^{*\top} = W_i^{*\top} H^*$. Since $W_i^* \in \Delta^{K-1}$, it follows that $Y_i^* \in \text{conv}(\mathcal{H}^*)$ and so

$$S_n = \text{conv}\{Y_1^*, \dots, Y_n^*\} \subset \text{conv}(\mathcal{H}^*).$$

Thus the Hausdorff distance reduces to the directed distance

$$d_{\text{Haus}}(S_n, \text{conv}(\mathcal{H}^*)) = \sup_{y \in \text{conv}(\mathcal{H}^*)} \text{dist}(y, S_n).$$

Fix $\epsilon > 0$. By Assumption 2, for each vertex e_k of Δ^{K-1} , there exists $c_k > 0$ such that any open ball around $c_k e_k$ has positive mass under \mathbb{P}_W . Choose $\epsilon' < \min\left[\frac{c_k}{2\sqrt{K}}, \frac{\epsilon c_k}{2(1+\sqrt{K})}\right]$. Consider any vector $w \in \mathbb{R}_+^K \sim \mathbb{P}_W$ with $\|w - c_k e_k\| \leq \epsilon'$ for any k . Then, by Cauchy-Schwarz,

$$|1_K^\top w - c_k| = |1_K^\top (w - c_k e_k)| \leq \|1_K\| \|w - c_k e_k\| \leq \sqrt{K} \epsilon'.$$

Hence $1_K^\top w \geq c_k - \sqrt{K} \epsilon' \geq \frac{c_k}{2}$, implying

$$\frac{1}{1_K^\top w} \leq \frac{2}{c_k}.$$

Define the normalized vector $w^* = w/(1_K^\top w) \in \Delta^{K-1}$. Then, inserting the above bounds,

$$\|w^* - e_k\| = \left\| \frac{w}{1_K^\top w} - \frac{c_k e_k}{c_k} \right\| \leq \frac{\|w - c_k e_k\|}{1_K^\top w} + \frac{|1_K^\top w - c_k|}{1_K^\top w} \leq \frac{2\epsilon'}{c_k} + \frac{2\sqrt{K}\epsilon'}{c_k} = \frac{2(1 + \sqrt{K})\epsilon'}{c_k} \leq \epsilon.$$

Because $\mathbb{P}_W(B(c_k e_k, \epsilon')) > 0$ where $B(c_k e_k, \epsilon')$ is the open ball of radius ϵ' centered at $c_k e_k$, continuity of the normalization map $w \mapsto w/(1_K^\top w)$ and the bound above imply

$$\mathbb{P}_{W^*}(B(e_k, \epsilon)) > 0.$$

Thus $e_k \in \mathcal{A}$ for every k .

Fix $\varepsilon > 0$ and set $\delta = \varepsilon/\|H^*\|_{\text{op}}$. Here, the operator norm $\|H^*\|_{\text{op}}$ is non-zero because $H^* = D^{-1}H$, in which H is a full row rank matrix and D is a diagonal matrix with positive entries. For any $y \in \text{conv}(\mathcal{H}^*)$, write $y^\top = w^{*\top} H^*$ with $w^* \in \Delta^{K-1}$.

Because each e_k is in the support of \mathbb{P}_{W^*} , $p_k = \mathbb{P}_{W^*}(B(e_k, \delta)) > 0$. By Birkhoff's ergodic theorem, $\frac{1}{n} \sum_{i=1}^n I\{W_i^* \in B(e_k, \delta)\} \rightarrow p_k$ almost surely, so the set of times $\{i : W_i^* \in B(e_k, \delta)\}$ is infinite almost surely as $n \rightarrow \infty$. Define $i_k(n) = \max\{i \leq n : W_i^* \in B(e_k, \delta)\}$. Then by Birkhoff's theorem $i_k(n) \leq n$ is defined for all $k = 1, \dots, K$ for any $n \geq$ some $N(\varepsilon)$, and $W_{i_k(n)}^* \in B(e_k, \delta)$. Consider the following estimate of y :

$$\hat{y}_n(y) = \sum_{k=1}^K w_k^* Y_{i_k(n)}^* \in S_n.$$

Then, for any $n \geq N(\varepsilon)$

$$\begin{aligned} \|y - \hat{y}_n(y)\| &\leq \sum_{k=1}^K w_k^* \|e_k^\top H^* - W_{i_k(n)}^{*\top} H^*\| \\ &\leq \sum_{k=1}^K w_k^* \|e_k - W_{i_k(n)}^*\| \|H^*\|_{\text{op}} \\ &\leq \delta \|H^*\|_{\text{op}} \sum_{k=1}^K w_k^* = \delta \|H^*\|_{\text{op}} = \varepsilon. \end{aligned}$$

Hence for every $y \in \text{conv}(\mathcal{H}^*)$, $\text{dist}(y, S_n) < \varepsilon$ for all $n \geq N(\varepsilon)$, almost surely. The result holds uniformly over all $y \in \text{conv}(\mathcal{H})$ as $N(\varepsilon)$ only depends on ε and $\|H\|_{\text{op}}$.

So for any $\varepsilon > 0$, we have for all $n \geq N(\varepsilon)$,

$$\sup_{y \in \text{conv}(\mathcal{H}^*)} \text{dist}(y, S_n) < \varepsilon \quad \text{almost surely.}$$

As mentioned before, since $S_n \subset \text{conv}(\mathcal{H}^*)$, this directed distance is exactly $d_{\text{Haus}}(S_n, \text{conv}(\mathcal{H}^*))$. We have shown that this goes to zero almost surely and the proof of Theorem 2 is complete. \square

Proof of Corollary 1. By Theorem 2, $S_n \rightarrow \text{conv}(\mathcal{H}^*)$ almost surely in the Hausdorff distance. Because all these sets lie in a fixed compact ball of \mathbb{R}^J , the product spaces S_n^K and $\text{conv}(\mathcal{H}^*)^K$ are compact.

For $V = (v_1, \dots, v_K) \in \mathbb{R}^{J \times K}$, define

$$G(V) = \text{vol}_{K-1}(\text{conv}\{v_1, \dots, v_K\}).$$

The map $V \mapsto \text{conv}\{v_1, \dots, v_K\}$ is continuous under the Hausdorff metric, and the $(K-1)$ -dimensional volume vol_{K-1} is continuous on compact sets. Hence G is continuous on $\mathbb{R}^{J \times K}$.

For any $v_1, \dots, v_K \in \text{conv}(\mathcal{H}^*)$, $\text{conv}\{v_1, \dots, v_K\} \subset \text{conv}(\mathcal{H}^*)$, so $G(v) \leq \text{vol}_{K-1}(\text{conv}(\mathcal{H}^*))$. Equality holds if and only if $\text{conv}\{v_1, \dots, v_K\} = \text{conv}(\mathcal{H}^*)$. Since $\text{conv}(\mathcal{H}^*)$ has exactly K vertices, and the extreme points of a convex hull must belong to the generating set, the only K -point set in $\text{conv}(\mathcal{H}^*)$ whose convex hull equals $\text{conv}(\mathcal{H}^*)$ are the vertex sets $\{h_1^*, \dots, h_K^*\}$ up to permutation. Thus the maximizers of G on $\text{conv}(\mathcal{H}^*)^K$ are exactly the $K!$ permutations of $\{h_1^*, \dots, h_K^*\}$.

For each $k = 1, \dots, K$ choose $h_{n,k} \in S_n$ so that $\|h_{n,k} - h_k^*\| \rightarrow 0$. This is possible because $S_n \rightarrow \text{conv}(\mathcal{H}^*)$ almost surely in Hausdorff distance by Theorem 2. By continuity of G , we have $G(h_{n,1}, \dots, h_{n,K}) \rightarrow G(h_1^*, \dots, h_K^*) = \text{vol}_{K-1}(\text{conv}(\mathcal{H}^*))$. Let $\{\hat{h}_1^*, \dots, \hat{h}_K^*\}$ be any K -point subset of S_n that achieves maximum volume. Then we have

$$\liminf_{n \rightarrow \infty} G(\hat{h}_1^*, \dots, \hat{h}_K^*) \geq \lim_{n \rightarrow \infty} G(h_{n,1}, \dots, h_{n,K}) = \text{vol}_{K-1}(\text{conv}(\mathcal{H}^*)).$$

But the left-hand side cannot exceed $\text{vol}_{K-1}(\text{conv}(\mathcal{H}^*))$, so

$$G(\hat{h}_1^*, \dots, \hat{h}_K^*) \rightarrow \text{vol}_{K-1}(\text{conv}(\mathcal{H}^*)) \quad \text{almost surely.}$$

To make the dependence of \hat{h}_k^* on n explicit, we write them as $\hat{h}_{n,k}^*$. By compactness of $\text{conv}(\mathcal{H}^*)^K$, any subsequence of $\{\hat{h}_{n,1}^*, \dots, \hat{h}_{n,K}^*\}$ has a further subsequence converging to some $v = (v_1, \dots, v_K) \in \text{conv}(\mathcal{H}^*)^K$. By continuity of G and the previous convergence conclusion, $G(v) = \text{vol}_{K-1}(\text{conv}(\mathcal{H}^*))$. Therefore, the unordered set $\{v_1, \dots, v_K\}$ must equal $\{h_1^*, \dots, h_K^*\}$ by

the equality argument above. Since every convergent subsequence of $\{\hat{h}_{n,1}^*, \dots, \hat{h}_{n,K}^*\}$ has a further subsequence converging to the true vertex set,

$$d_{\text{Haus}}\left(\{\hat{h}_{n,1}^*, \dots, \hat{h}_{n,K}^*\}, \{h_1^*, \dots, h_K^*\}\right) \rightarrow 0 \quad \text{almost surely,}$$

which implies $\hat{H}^* \rightarrow H^*$ up to row permutations. \square

Proof of Proposition 1. By stationarity and ergodicity, the column mean \bar{Y}_n and its sum \bar{r}_n satisfy

$$(\bar{Y}_n, \bar{r}_n) \rightarrow (\mathbb{E}(Y_1), \mathbb{E}(r_1)) \quad \text{almost surely,}$$

where $r_i = Y_i^\top 1_J$. This leads to $(\bar{Y}_n, \bar{r}_n) \rightarrow (\mathbb{E}(Y_1), \mathbb{E}(r_1))$ in probability.

For any matrix $V \in \mathbb{R}^{K \times J}$, let $\bar{V} = [V \ 1_K]$ and define

$$R(V) = \bar{V}^\top (\bar{V} \bar{V}^\top)^+.$$

Then for any full row-rank $V \in \mathbb{R}^{K \times J}$, we have

$$R(V) = \bar{V}^\top (\bar{V} \bar{V}^\top)^{-1}, \quad \bar{V} R(V) = I_K.$$

Recall that $H \in \mathbb{R}^{K \times J}$ has full row rank and let $d := H 1_J$ have all entries nonzero. Set $D := \text{diag}(d)$ and $H^* := D^{-1}H$. We first show that the rows of H^* are affinely independent. Take any $\alpha \in \mathbb{R}^K$ with $\alpha^\top 1_K = 0$ and $\alpha^\top H^* = 0_J^T$. Define $\beta := D^{-1}\alpha$. Then

$$\beta^\top H = \alpha^\top D^{-1}H = \alpha^\top H^* = 0_J^T.$$

Since H has full row rank, $\beta = 0_K$. As D is a diagonal matrix with positive entries, we have $\alpha = D\beta = 0_K$. Therefore the rows of H^* are affinely independent. As each row of H^* satisfies $1_J^\top h_k^* = 1$, these K points lie in the affine hyperplane $\{x \in \mathbb{R}^J : 1_J^\top x = 1\}$ and have affine rank $K-1$.

Next we show that \bar{H}^* is full row rank. Take any $\alpha \in \mathbb{R}^K$ with $\alpha^\top \bar{H}^* = 0_J^T$. Then

$$\alpha^\top H^* = 0_J^T \quad \text{and} \quad \alpha^\top 1_K = 0.$$

By affine independence of the rows of H^* , the conditions $\alpha^\top H^* = 0_J^T$ and $\alpha^\top 1_K = 0$ imply $\alpha = 0_K$. Hence the rows of \bar{H}^* are linearly independent and $\text{rank}(\bar{H}^*) = K$.

So $\bar{H}^* \bar{H}^{*\top}$ is invertible, and the map $R(\cdot)$ is continuous in a neighborhood of \bar{H}^* . By the continuous mapping theorem,

$$\hat{H}^* \rightarrow H^* \quad \text{in probability} \implies R(\hat{H}^*) \rightarrow R(H^*) \quad \text{in probability.}$$

Recall that

$$\mathbb{E}(Y_1^\top) = \tilde{\mu}^\top H^*, \quad \mathbb{E}(r_1) = \mathbb{E}(Y_1^\top) 1_J = \tilde{\mu}^\top H^* 1_J = \tilde{\mu}^\top 1_K.$$

Hence

$$[\mathbb{E}(Y_1^\top) \ \mathbb{E}(r_1)] R(H^*) = [\tilde{\mu}^\top H^* \ \tilde{\mu}^\top 1_K] R(H^*) = \tilde{\mu}^\top \bar{H}^* R(H^*) = \tilde{\mu}^\top I_K = \tilde{\mu}^\top.$$

Define the estimator $\tilde{m}_n^\top = [\bar{Y}_n^\top \ \bar{r}_n] R(\hat{H}^*)$. Combining the previous convergence in probability results and applying the continuous mapping theorem (matrix multiplication is continuous),

$$\tilde{m}_n^\top = [\bar{Y}_n^\top \ \bar{r}_n] R(\hat{H}^*) \rightarrow [\mathbb{E}(Y_1^\top) \ \mathbb{E}(r_1)] R(H^*) = \tilde{\mu}^\top \quad \text{in probability,}$$

i.e. $\tilde{m}_n \rightarrow \tilde{\mu}$ in probability. The almost-sure version follows identically. \square

Algorithm 2 DETAILED ALGORITHM FOR SOURCE ATTRIBUTION PERCENTAGE MATRIX ESTIMATION

Input: $Y \in \mathbb{R}_+^{n \times J}$, number of sources $K < J$, optional pruning flag, tolerances ε .

Output: $\hat{\Phi}$

- 1: **Row normalization:** set $r \leftarrow Y1_J$ and $Y^* \leftarrow (\text{diag}(r))^{-1} Y$.
- 2: **Intrinsic projection:** set $Y_{\text{red}} \leftarrow Y^*[:, 1:J-1]$; compute the column-means $m_{\text{red}} \leftarrow \frac{1}{n} 1_n^\top Y_{\text{red}}$; center $Y_c \leftarrow Y_{\text{red}} - 1_n m_{\text{red}}^\top$; compute thin SVD $Y_c = U \Sigma V^\top$ and take $B \leftarrow V[:, 1:r_B]$ with rank r_B ; finally set $Z \leftarrow Y_c B$.
- 3: **Hull vertices:** compute convex hull of Z ; let $\mathcal{I}_{\text{hull}}$ be its vertex indices; set $H_{\text{cand}}^* \leftarrow Y^*[\mathcal{I}_{\text{hull}}, :]$.
- 4: **if** pruning enabled **then**
- 5: cluster H_{cand}^* (e.g., mini-batch k -means); keep one representative per cluster to obtain pruned H_{cand}^* .
- 6: **end if**
- 7: **Max-volume selection (global search):** for each K -subset $S \subset H_{\text{cand}}^*$, compute its intrinsic $(K-1)$ -volume $\log V(S)$; choose $S^* = \arg \max_S \log V(S)$ and set $\hat{H}^* \leftarrow S^*$. (*Alternatively, approximate the maximizer via an N-FINDR-style greedy search.*)
- 8: **Affine right-inverse:** augment $\hat{H}_{\text{aug}}^* \leftarrow [\hat{H}^* \ 1_K]$, $Y_{\text{aug}}^* \leftarrow [Y^* \ 1_n]$; compute $R(\hat{H}^*) \leftarrow \text{pinv}(H_{\text{aug}})$ and $W_{\text{raw}}^* \leftarrow Y_{\text{aug}}^* R(\hat{H}^*)$.
- 9: **Simplex projection:** replace entries of W_{raw}^* by $\max(W_{\text{raw}}^*, \varepsilon)$ for small $\varepsilon > 0$, then normalize each row to sum 1; denote result by \hat{W}^* .
- 10: **Sample mean:** compute \tilde{m}_n as the column means of $\text{diag}(r)\hat{W}^*$.
- 11: **Source attributions:** set

$$\hat{\phi}_{kj} \leftarrow \frac{\tilde{m}_{n,k} \hat{H}_{kj}^*}{\sum_{\ell=1}^K \tilde{m}_{n,\ell} \hat{H}_{\ell j}^*}, \quad k = 1, \dots, K, \quad j = 1, \dots, J.$$

- 12: **Return** $\hat{\Phi}$.

S2 Detailed algorithm

S3 Numerical experiments

S3.1 Stationary ergodic process W

We simulate an $n \times J$ non-negative data matrix Y as $Y = WH$, with $W \in \mathbb{R}_+^{n \times K}$ and $H \in \mathbb{R}_+^{K \times J}$. We set $J = 8$ and $K = 3$. We construct H as follows. A large set of candidate vectors in \mathbb{R}^J is sampled with independent and identically distributed (iid) entries from an $\text{Exp}(1)$ distribution. The convex hull of the candidate set is then computed, and K of its vertices are selected to form the rows of H . We generate W from a log-autoregressive process of order one (log-AR(1)). For each $k \in \{1, \dots, K\}$, we simulate a stationary Gaussian AR(1) on $g_{ik} = \log W_{ik}$:

$$g_{ik} = \mu_k^{(g)} + \phi_k(g_{i-1,k} - \mu_k^{(g)}) + \varepsilon_{ik}, \quad \varepsilon_{ik} \sim \mathcal{N}(0, \sigma_{\varepsilon,k}^2), \quad |\phi_k| < 1,$$

initialized at stationarity $g_{1k} \sim \mathcal{N}(\mu_k^{(g)}, \sigma_{\varepsilon,k}^2 / (1 - \phi_k^2))$. Exponentiation yields non-negative factors $W_{ik} = \exp(g_{ik})$ with stationary lognormal marginals. The corresponding population mean is

$$\mu_k = \mathbb{E}(W_{ik}) = \exp\left(\mu_k^{(g)} + \frac{1}{2} \frac{\sigma_{\varepsilon,k}^2}{1 - \phi_k^2}\right).$$

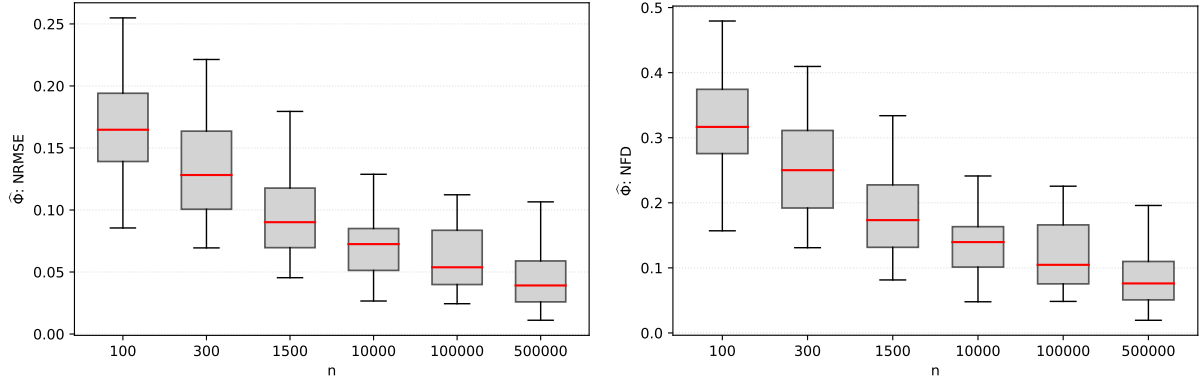


Figure S1: Box plots of NRMSE (left) and NFD (right) for $\hat{\Phi}$ over 50 replicates as a function of n . The boxes display the interquartile range with median (red line) and whiskers to the minimum and maximum after outlier removal.

The autoregressive coefficient is fixed at $\phi_k = 0.8$ for all k , imposing strong temporal correlation in the data. The location and scale parameters of the latent Gaussian innovations are randomly drawn as $\mu_k^{(g)} \sim \text{Unif}(-0.5, 0.5)$ and $\sigma_{\varepsilon,k} \sim \text{Unif}(0.15, 0.5)$, respectively. We vary $n \in \{100, 300, 1500, 10000, 100000, 500000\}$ and, for each n , repeat the data generation and estimation 50 times.

We implement both a greedy and an exhaustive search for the K vertices with maximum simplex volume. The greedy search is initialized by the Automatic Target Generation Process and iteratively replaces a vertex while the simplex volume increases. The exhaustive search evaluates the volume for all K -tuples and returns the one with the maximum volume. The exhaustive search is only feasible for small n due to its computational cost. For $n \in \{100, 300\}$, both searches yield indistinguishable accuracy and similar runtimes for estimating Φ . Hence, we report results from the greedy search in this section.

Let $(\hat{\phi}_{kj})$ denote an estimate for Φ after permuting rows to minimize the total Euclidean distance between the true and estimated rows. We use normalized root mean squared error (NRMSE), and normalized Frobenius distance (NFD) as performance measures, defined in Table S1.

Table S1: Performance measures for source attribution percentage matrix estimates.

Metric	Formula
NRMSE	$\frac{1}{K} \sum_{k=1}^K \left(\frac{\sqrt{\frac{1}{J} \sum_{j=1}^J (\hat{\phi}_{kj} - \phi_{kj})^2}}{\ \phi_{k\cdot}\ _2} \right)$
NFD	$\ \Phi - \hat{\Phi}\ _F / \ \Phi\ _F$

Figure S1 summarizes NRMSE and NFD across replicates for varying n . Both error metrics decrease monotonically with n . The mean NRMSE and NFD reach approximately 0.047 and 0.089, respectively, at the largest n . Scatter plots in Figure S2 show the estimated entries of $\hat{\Phi}$ aligning closely with the 45-degree line as n increases. The slight regression-to-the-mean bias (slopes below one) is expected because Φ is bounded in $[0,1]$ with column sums constrained to one.

For each sample size n we compare heat maps of the true Φ with the estimates $\hat{\Phi}$ (Figure S3) and display the estimated \hat{H}^* alongside the true H^* in pairwise scatter plots of the normalized data

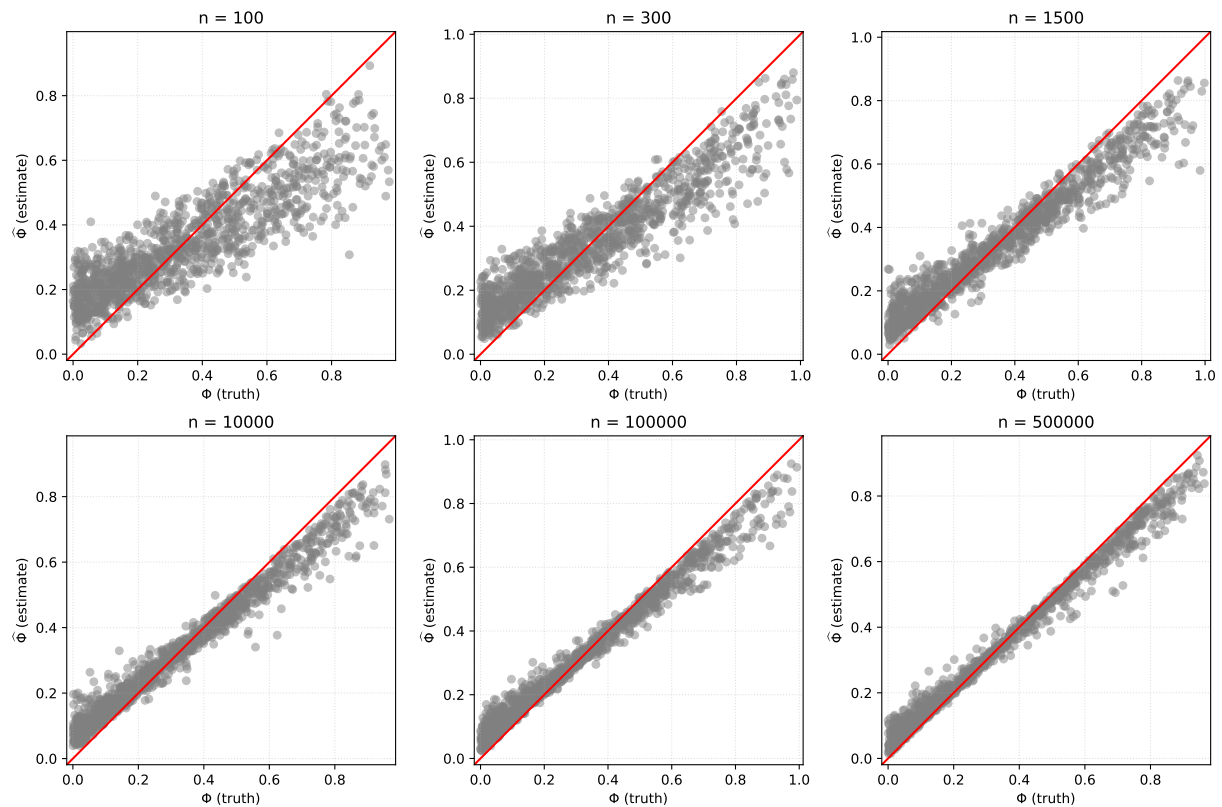


Figure S2: Scatter plots of the $K \times J = 24$ elements of true versus estimated Φ over 50 replicates, with the 45-degree line in red.

Y^* (Figures S4 – S6). To illustrate the trend we show results for $n \in \{300, 100000, 500000\}$ from a randomly chosen replicate. The figures indicate that as n increases, \widehat{H}^* and $\widehat{\Phi}$ converge visually to their true counterparts.

S3.2 Independent and identically distributed W

Our next set of simulations show robustness of the consistency result to a more complex (mixture) distribution generating the emissions. For this set of simulations, we fix $J = 10$ and $K = 5$ and assume W is iid across rows. Independently for each column $k \in \{1, \dots, K\}$, we specify a finite mixture on $\log W_{ik}$:

$$\log W_{ik} \mid Z_{ik} = c \sim \mathcal{N}(\mu_{kc}, \sigma_{kc}^2), \quad \text{pr}(Z_{ik} = c) = \pi_{kc},$$

with mixture components $C_k \sim \text{Pois}(3) + 1$, mixture weights $\pi_{k \cdot} \sim \text{Dirichlet}(1_{C_k})$, and component parameters $\mu_{kc} \sim \text{Unif}(-1, 1)$ and $\sigma_{kc} \sim \text{Unif}(0.1, 1)$. This yields strictly positive $W_{ik} = \exp(\log W_{ik})$. The population mean for column k is available in closed form,

$$\mu_k = \mathbb{E}(W_{ik}) = \sum_{c=1}^{C_k} \pi_{kc} \exp\left(\mu_{kc} + \frac{1}{2}\sigma_{kc}^2\right).$$

All other settings mirror Section S3.1. As J and K increase, the exhaustive search rapidly becomes intractable, whereas the greedy search is inexpensive and exhibits negligible loss in estimation accuracy. The box plots and scatter plots in Figures S7 – S8 support the theory of asymptotic convergence of $\widehat{\Phi}$ in the iid case.

References

Berman, A. and Plemmons, R. J. (1979). Chapter 2 - Nonnegative matrices. In Berman, A. and Plemmons, R. J., editors, *Nonnegative matrices in the mathematical sciences*, pages 26–62. Academic Press. URL: <https://www.sciencedirect.com/science/article/pii/B9780120922505500096>.

Brunel, V.-E. (2019). Uniform behaviors of random polytopes under the Hausdorff metric. *Bernoulli*, 25(3):1770–1793. DOI: <http://doi.org/10.3150/18-BEJ1035>.

Donoho, D. and Stodden, V. (2003). When does non-negative matrix factorization give a correct decomposition into parts? In *Advances in Neural Information Processing Systems*, volume 16. MIT Press. URL: https://papers.nips.cc/paper_files/paper/2003/hash/1843e35d41ccf6e63273495ba42df3c1-Abstract.html.

Du, B., Wang, S., Wang, N., Zhang, L., Tao, D., and Zhang, L. (2016). Hyperspectral signal unmixing based on constrained non-negative matrix factorization approach. *Neurocomputing*, 204:153–161. DOI: <http://doi.org/10.1016/j.neucom.2015.10.132>.

EPA, U. (2015). EPA Positive Matrix Factorization 5.0 fundamentals and user guide. URL: <https://www.epa.gov/air-research/epa-positive-matrix-factorization-50-fundamentals-and-user-guide>.

Fritzilas, E., Milanić, M., Rahmann, S., and Rios-Solis, Y. A. (2010). Structural identifiability in low-rank matrix factorization. *Algorithmica*, 56(3):313–332. DOI: <http://doi.org/10.1007/s00453-009-9331-2>.

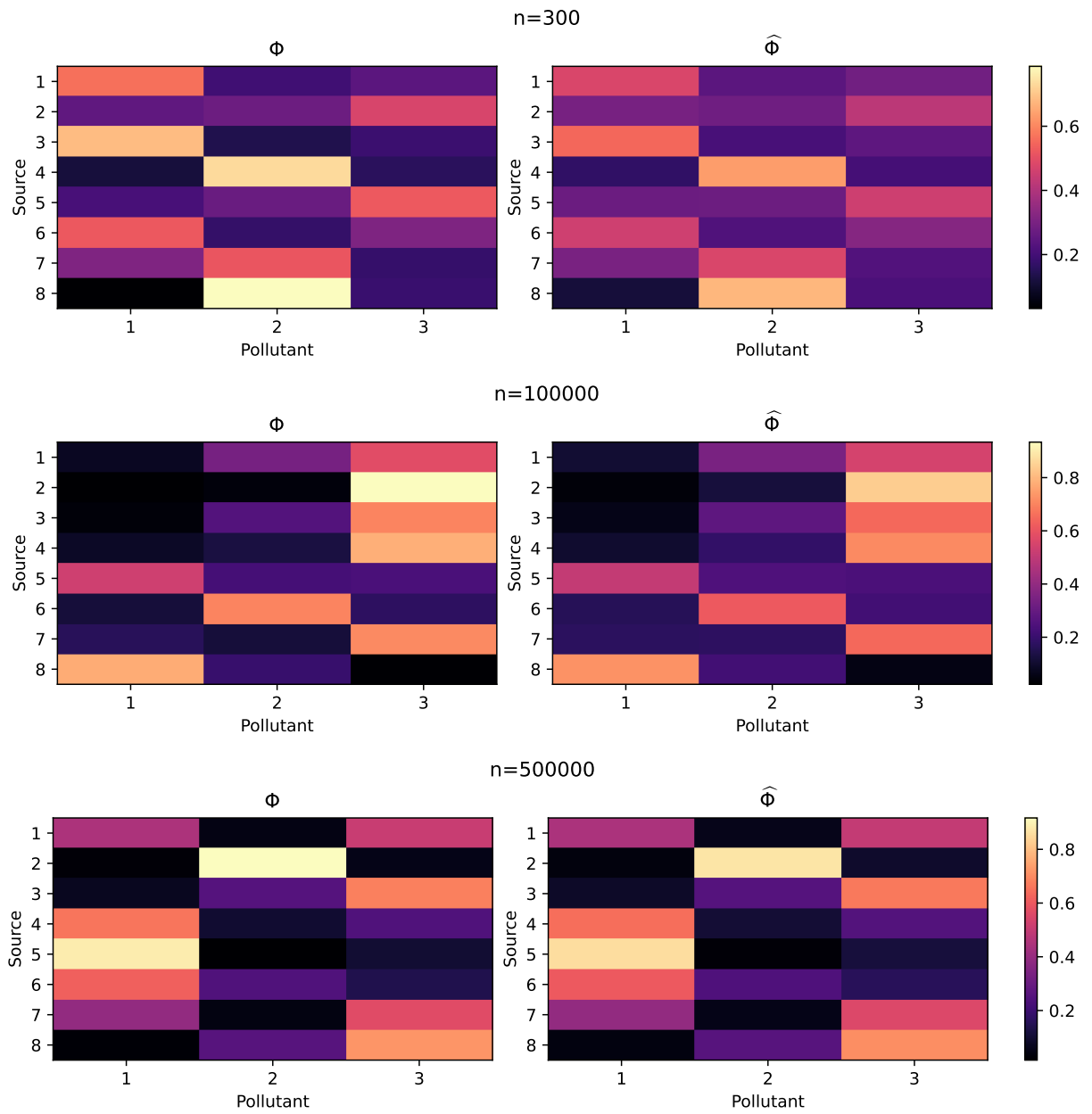


Figure S3: Heat maps of the true Φ (left) and the estimate $\hat{\Phi}$ (right) for a randomly selected replicate for $n = 300$ (top), $n = 100000$ (middle), and $n = 500000$ (bottom).

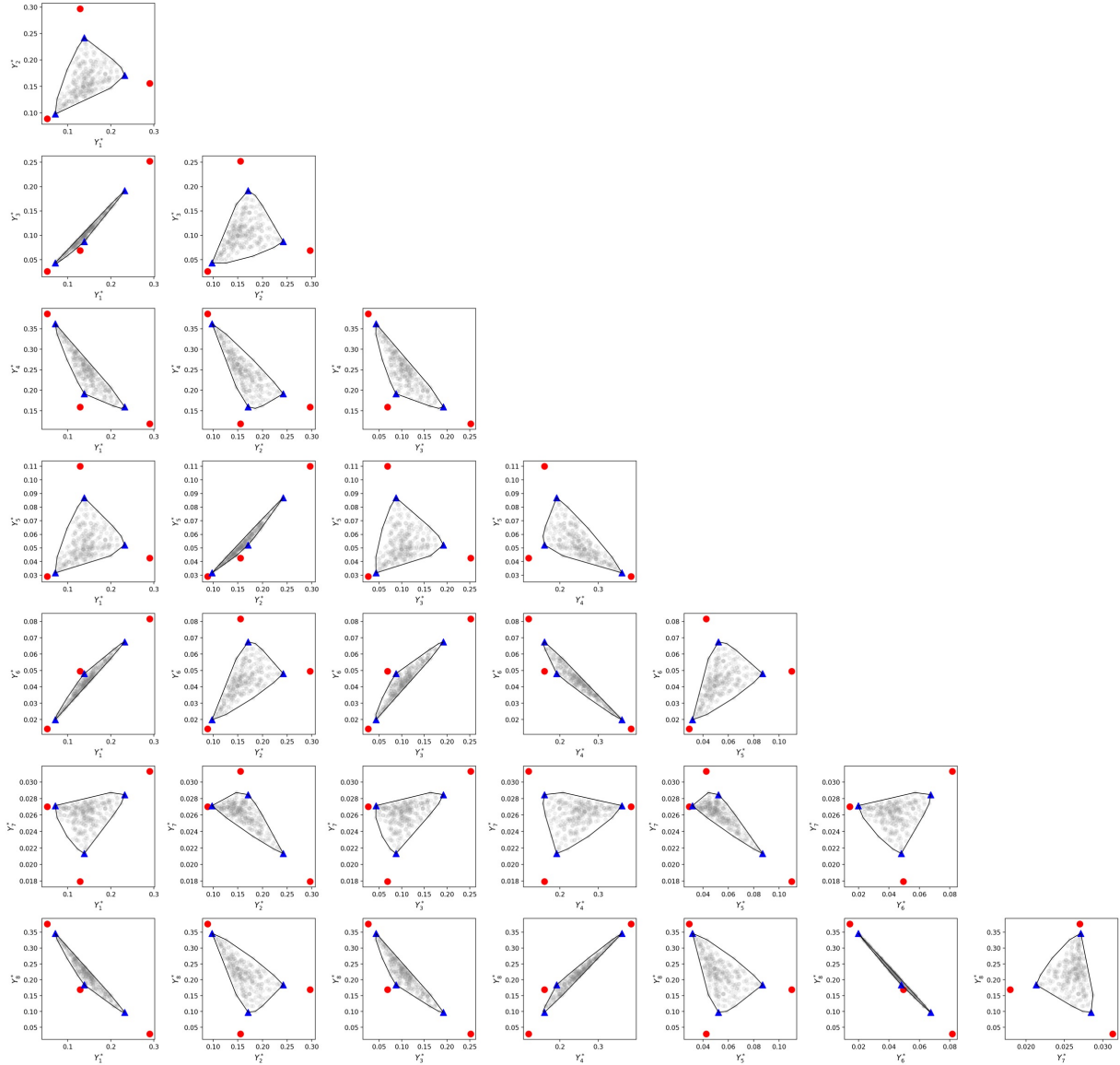


Figure S4: Sample hull of Y^* with the true H^* in red dots and the estimated \hat{H}^* in blue triangles for a randomly selected replicate for $n = 300$.

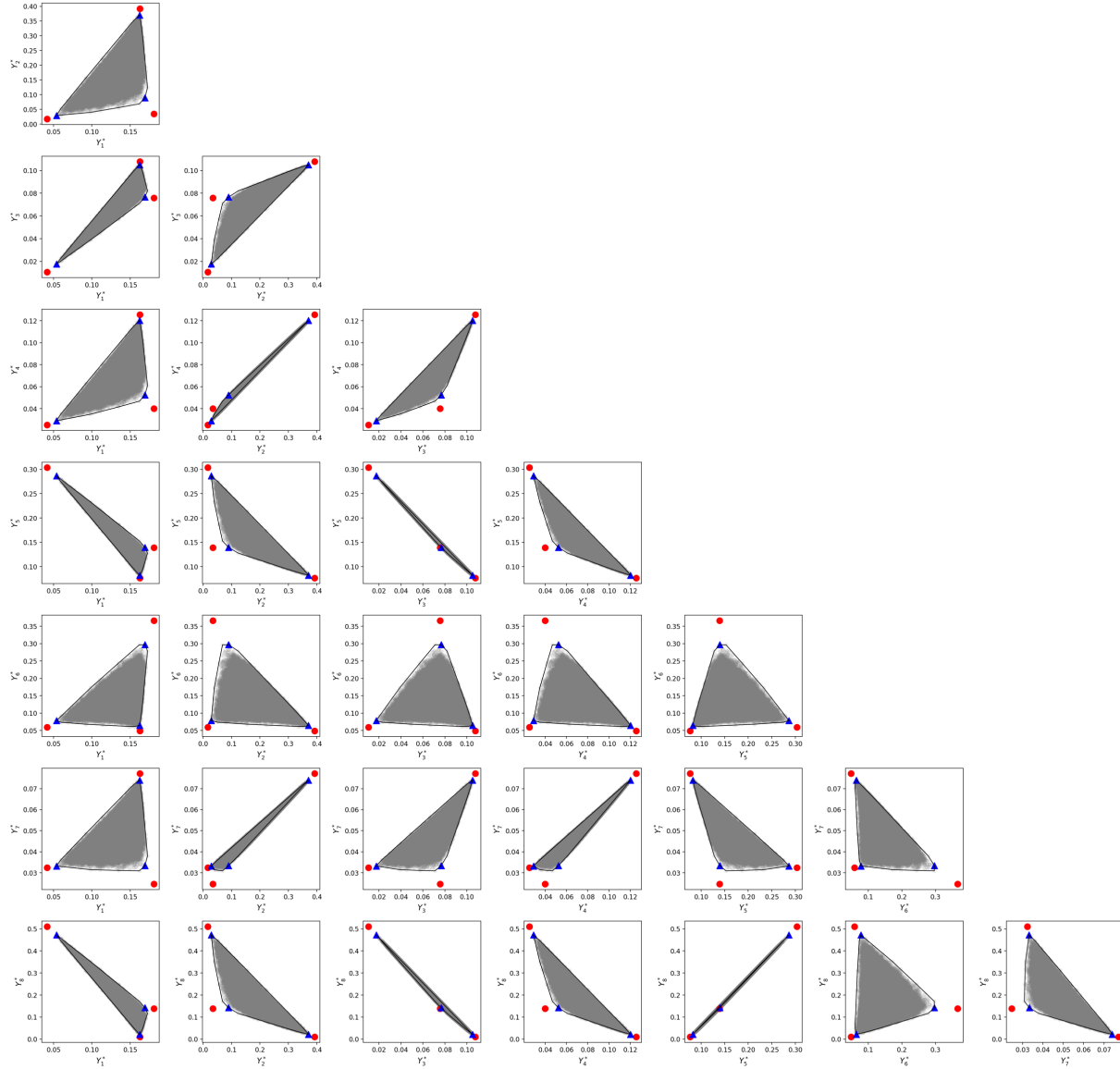


Figure S5: Sample hull of Y^* with the true H^* in red dots and the estimated \hat{H}^* in blue triangles for a randomly selected replicate for $n = 100000$.

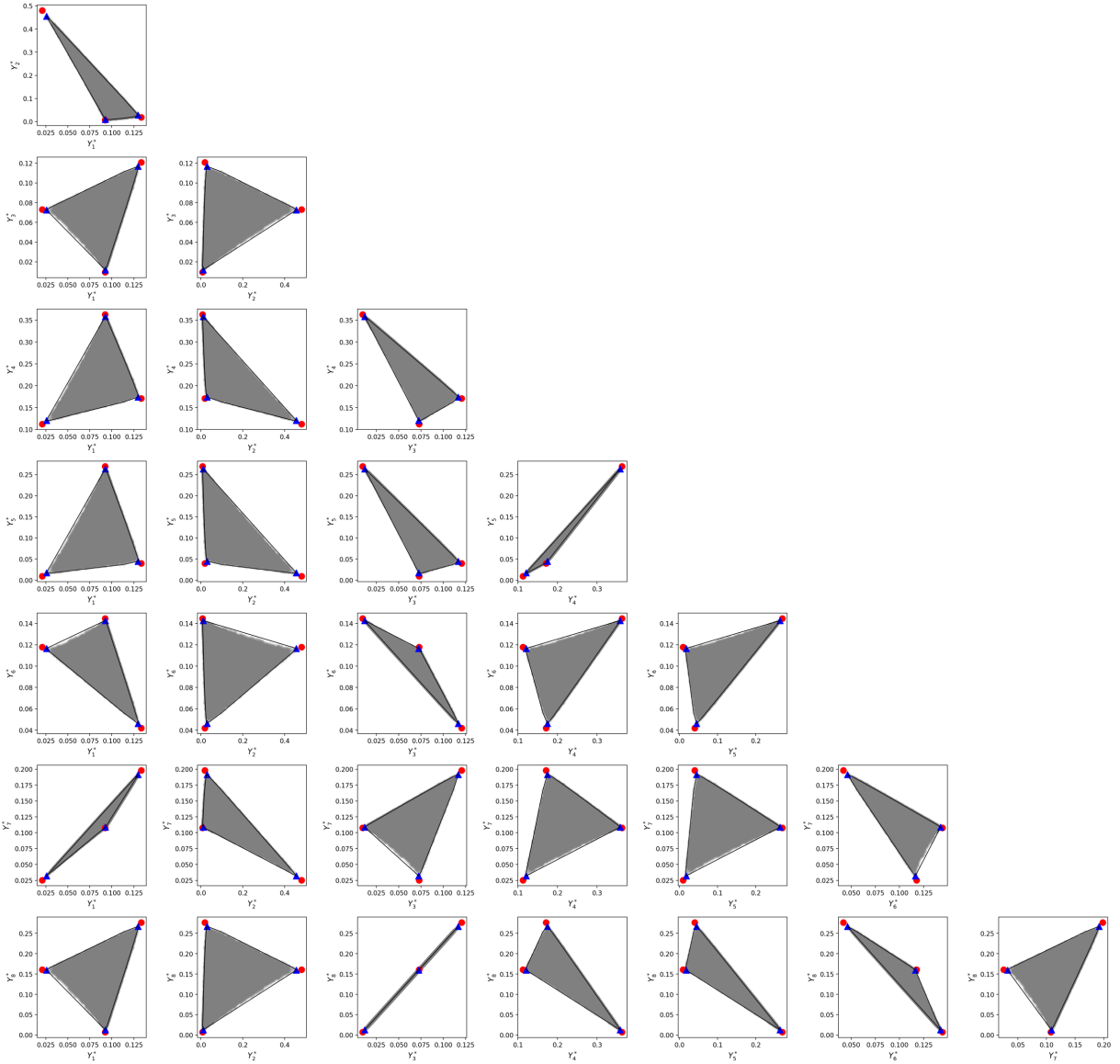


Figure S6: Sample hull of Y^* with the true H^* in red dots and the estimated \hat{H}^* in blue triangles for a randomly selected replicate for $n = 500000$.

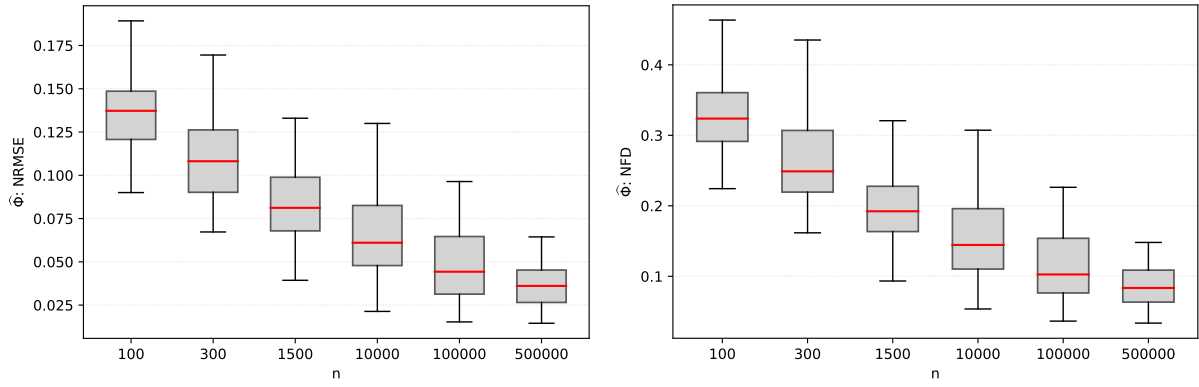


Figure S7: Box plots of NRMSE (left) and NFD (right) for $\hat{\Phi}$ over 50 replicates in the iid W setting.

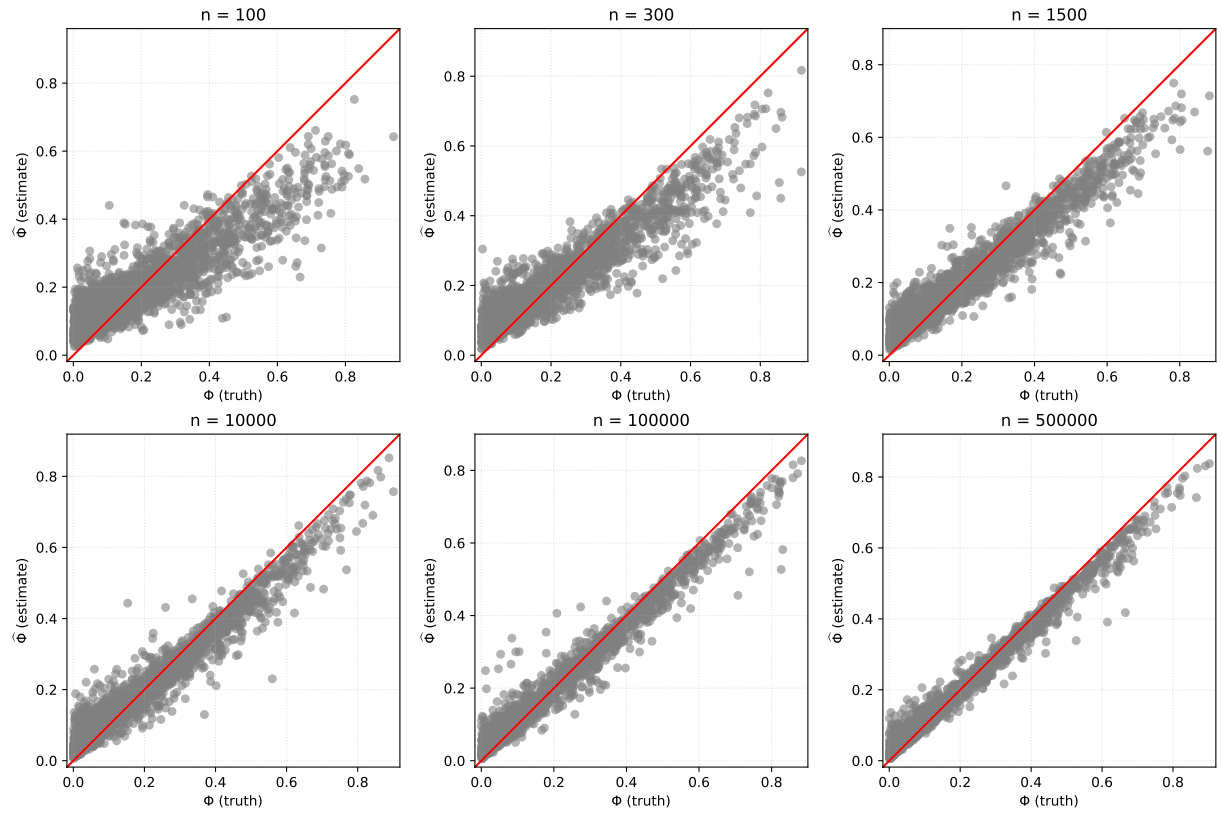


Figure S8: Scatter plots of $K \times J = 50$ elements of true versus estimated Φ over 50 replicates in the iid W setting, with the 45-degree line in red.

Fu, X., Huang, K., and Sidiropoulos, N. D. (2018). On identifiability of nonnegative matrix factorization. *IEEE Signal Processing Letters*, 25(3):328–332. DOI: <http://doi.org/10.1109/LSP.2018.2789405>.

Gillis, N. (2017). Introduction to nonnegative matrix factorization. DOI: <http://doi.org/10.48550/arXiv.1703.00663>.

Hackstadt, A. J. and Peng, R. D. (2014). A Bayesian multivariate receptor model for estimating source contributions to particulate matter pollution using national databases. *Environmetrics*, 25(7):513–527. DOI: <http://doi.org/10.1002/env.2296>.

Hagan, D. H., Gani, S., Bhandari, S., Patel, K., Habib, G., Apte, J. S., Hildebrandt Ruiz, L., and Kroll, J. H. (2019). Inferring Aerosol sources from low-cost air quality sensor measurements: a case study in Delhi, India. *Environmental Science & Technology Letters*, 6(8):467–472. DOI: <http://doi.org/10.1021/acs.estlett.9b00393>.

Henry, R. C. (1997). History and fundamentals of multivariate air quality receptor models. *Chemometrics and Intelligent Laboratory Systems*, 37(1):37–42. DOI: [http://doi.org/10.1016/S0169-7439\(96\)00048-2](http://doi.org/10.1016/S0169-7439(96)00048-2).

Jun, M. and Park, E. S. (2013). Multivariate receptor models for spatially correlated multipollutant data. *Technometrics*, 55(3):309–320. DOI: <http://doi.org/10.1080/00401706.2013.765321>.

Kallel, S. and Louhichi, S. (2024). Topological reconstruction of compact supports of dependent stationary random variables. *Advances in Applied Probability*, 56(4):1339–1369. DOI: <http://doi.org/10.1017/apr.2024.4>.

Krall, J. R. and Chang, H. H. (2019). Statistical methods for source apportionment. In *Handbook of Environmental and Ecological Statistics*. Chapman and Hall/CRC.

Kumar, A., Sindhwan, V., and Kambadur, P. (2013). Fast Conical Hull Algorithms for Near-separable Non-negative Matrix Factorization. In *Proceedings of the 30th International Conference on Machine Learning*, pages 231–239. PMLR. URL: <https://proceedings.mlr.press/v28/kumar13b.html>.

Louhichi, S. (2025). Sharp rates of convergence in the Hausdorff metric for some compactly supported stationary sequences. *Journal of Applied Probability*, pages 1–29. DOI: <http://doi.org/10.1017/jpr.2025.7>.

Manousakas, M., Rausch, J., Jaramillo-Vogel, D., Schneider-Beltran, K. S., Alastuey, A., Jaffrezo, J.-L., Uzu, G., Persegues, S., Schnidrig, N., Prevot, A. S. H., and Daellenbach, K. R. (2025). Comparison of PM source profiles identified by different techniques and the potential of utilizing single-particle analysis data in source apportionment. *Atmospheric Environment: X*, 27:100363. DOI: <http://doi.org/10.1016/j.aaea.2025.100363>.

Nascimento, J. and Dias, J. (2005). Vertex component analysis: a fast algorithm to unmix hyperspectral data. *IEEE Transactions on Geoscience and Remote Sensing*, 43(4):898–910. DOI: <http://doi.org/10.1109/TGRS.2005.844293>.

Paatero, P. and Tapper, U. (1994). Positive matrix factorization: A non-negative factor model with optimal utilization of error estimates of data values. *Environmetrics*, 5(2):111–126. DOI: <http://doi.org/10.1002/env.3170050203>.

Park, E. S., Guttorp, P., and Henry, R. C. (2001). Multivariate receptor modeling for temporally correlated data by using MCMC. *Journal of the American Statistical Association*, 96(456):1171–1183. DOI: <http://doi.org/10.1198/016214501753381823>.

Sug Park, E., Spiegelman, C. H., and Henry, R. C. (2002). Bilinear estimation of pollution source profiles and amounts by using multivariate receptor models. *Environmetrics*, 13(7):775–798. DOI: <http://doi.org/10.1002/env.557>.

Viana, M., Kuhlbusch, T. A. J., Querol, X., Alastuey, A., Harrison, R. M., Hopke, P. K., Winiwarter, W., Vallius, M., Szidat, S., Prévôt, A. S. H., Hueglin, C., Bloemen, H., Wåhlin, P., Vecchi, R., Miranda, A. I., Kasper-Giebl, A., Maenhaut, W., and Hitzenberger, R. (2008). Source apportionment of particulate matter in Europe: A review of methods and results. *Journal of Aerosol Science*, 39(10):827–849. DOI: <http://doi.org/10.1016/j.jaerosci.2008.05.007>.

Winter, M. E. (1999). N-FINDR: an algorithm for fast autonomous spectral end-member determination in hyperspectral data. In *Imaging Spectrometry V*, volume 3753, pages 266–275. SPIE. DOI: <http://doi.org/10.1117/12.366289>.